J|A|C|S ARTICLES

Published on Web 08/24/2009

Modeling Dinitrogen Activation by Lithium: A Mechanistic Investigation of the Cleavage of N_2 by Stepwise Insertion into Small Lithium Clusters

Debjani Roy,[†] Armando Navarro-Vazquez,[‡,§] and Paul. v. R. Schleyer*[,†]

Center for Computational Chemistry, Department of Chemistry, University of Georgia, Athens, Georgia 30602, Departamento de Química Orgánica, Universidade de Santiago de Compostela, 15706 Santiago de Compostela, Spain, and Departamento de Química Orgánica, Universidade de Vigo, 36310 Vigo, Spain

Received April 14, 2009; E-mail: schleyer@chem.uga.edu

Abstract: Because of the inertness of molecular nitrogen, its practicable activation under mild conditions is a fundamental challenge. Nature can do it easily; chemists should be able to achieve comparable success. Lithium is exceptional among the main group elements in that it slowly reacts with N_2 at room temperature, leading finally to $(NLi_3)_n$, lithium nitride, a product of interest in its own right, because of its potential as a hydrogen storage medium. We explored this remarkably facile dinitrogen activation reaction by using model lithium clusters. Our extensive computations elucidate mechanisms for the ready reactions of N_2 with various model clusters, Li_2, Li_4, Li_6, and Li_8, leading to stepwise cleavage of the NN bond during dinitrogen reduction, N_2^0 to 2 N^{3-}. Initial isomeric N_2-Li_n complexes, retaining NN triple bonds, undergo cluster insertion/reduction processes over generally low barriers. A minimum of eight lithium atoms are needed to cleave the triple bonded nitrogen completely in a highly exothermic process. Moreover, we provide an explanation for the exceptional reactivity of N_2 with Li, compared to the other alkali metals, e.g., Na and K. Li is a very strong reducing agent as its nitrides have the highest atomization energy, the shortest M−N bond distance, and the largest M−N charge separation as well as interaction energy. Our study delineates the general manner in which molecular nitrogen can be activated sequentially by electron transfer and bond elongation, to give a series of increasingly reduced complexes. We conclude that lithium incorporation into complexes might facilitate the development of nitrogen fixation catalysts.

1. Introduction

Nitrogen, in addition to the noble gases, is the most inert chemical element. N_2 is a nonpolar molecule with tightly bound σ and π electrons and is very difficult to reduce due to its very large bond dissociation energy (224.5 kcal/mol), highly negative electron affinity (−1.8 eV), and huge HOMO/LUMO energy gap (22.9 eV).[1,2] Moreover, N_2 has a high ionization potential (15.0 eV) and does not donate electrons either.[1,2]

Reduction of dinitrogen remains a fundamental challenge for synthetic as well as theoretical chemistry. Unlike the catalytic Haber−Bosch hydrogenation of N_2 to give ammonia, which requires high pressure and high temperatures,[3] nitrogenase enzymes activate dinitrogen under ambient conditions at transition metal (Fe/MO, V)-sulfide cluster sites.[4] Metal complexes capable of cleaving the extremely robust dinitrogen triple bond are formed typically from low-valent early transition metal precursors. Since the first discovery of a dinitrogen complex in 1965, inorganic and organometallic chemists have contributed much fundamental knowledge on structures, binding modes, and reactivity patterns.[5] A plethora of dinitrogen complexes of transition metals, exhibiting different binding geometries of N_2 (end-on terminal, end-on bridging, side-on bridging, side-on end-on bridging), has been reported.[6] Most of these systems are highly covalent, with strong metal−nitrogen bonds. Moreover,

[†] University of Georgia.
[‡] Universidade de Santiago de Compostela.
[§] Universidade de Vigo.

(1) Johnson, S. A.; Fryzuk, M. D. *Coord. Chem. Rev.* **2000**, *200*, 379–409.
(2) Shaver, M. P.; Fryzuk, M. D. *Adv. Synth. Catal.* **2003**, *345*, 1061–1076.
(3) Smil, V. *Enriching the Earth: Fritz Haber, Carl Bosch and the Transformation of World Food Production*; The MIT Press: Cambridge, MA, 2001.
(4) (a) Hidai, M. *Coord. Chem. Rev.* **1999**, *85*, 99–108. (b) Leigh, G. J. *Acc. Chem. Res.* **1992**, *25*, 177–181. (c) Eady, R. R. *Chem. Rev.* **1996**, *96*, 3013–3030. (d) MacKey, B. A.; Fryzuk, M. D. *Chem. Rev.* **2004**, *104*, 385–401, and references therein.
(5) (a) Chertihin, G. V.; Andrews, L.; Bauschlicher, C. W. *J. Am. Chem. Soc.* **1998**, *120*, 3205–3212. (b) Chertihin, G. V.; Bare, W. D.; Andrews, L. *J. Phys. Chem. A* **1998**, *102*, 3697–3704. (c) Citra, A.; Andrews, L. *J. Am. Chem. Soc.* **1999**, *121*, 11567–11568. (d) Himmel, H. J.; Hubner, O.; Klopper, W.; Manceron, L. *Angew. Chem., Int. Ed.* **2000**, *45*, 2799–2802. (e) Tamelen, E. E.; Boche, G.; Ela, S. W.; Fechter, R. B. *J. Am. Chem. Soc.* **1967**, *89*, 5707. (f) Kuganathan, N.; Green, J. C.; Himmel, H. J. *New J. Chem.* **2006**, *30*, 1253–1261. (g) Zhou, M. F.; Jin, X.; Gong, Y.; Li, J. *Angew. Chem., Int. Ed.* **2007**, *46*, 2911–2914. (h) Himmel, H. J.; Reiher, M. *Angew. Chem., Int. Ed.* **2006**, *45*, 6264–6288. (i) Bonačić-Koutecký, V.; Fantucci, P.; Koutecký, J. *Chem. Rev.* **1991**, *91*, 1035–1108. (j) Li, J.; Li, S. *Angew. Chem., Int. Ed.* **2008**, *47*, 8040–8043. (k) Pool, J. A.; Lobkovsky, E.; Chirik, P. J. *Nature* **2004**, *427*, 527–530. (l) Spencer, L. P.; MacKay, B. A.; Patrick, B. O.; Fryzuk, M. D. *Proc. Natl. Acad. Sci. U.S.A.* **2006**, *103*, 17094–17098. (m) Akagi, F.; Matsuo, T.; Kawaguchi, H. *Angew. Chem., Int. Ed.* **2007**, *46*, 8778–8781.
(6) Studt, F.; Tuczek, F. *J. Comput. Chem.* **2006**, *27* (12), 1278–1291, and references therein.

there has been much recent progress, both practical and computational, in the field of synthetic nitrogen fixation.[7]

Lithium is exceptional among the main group elements as it reacts slowly with N_2 at room temperature to form lithium nitrides. Moreover lithium, in conjunction with transition metals, has been used to activate dinitrogen in several systems. Thus, in the presence of Li, a THF solution of $TiCl_4$ and TMSCl converts benzoyl chloride to $PhCONH_2$ in high yields at room temperature.[8] An intermediate complex of the $[TiX_m\{N(SiMe_3)_n\}_p]$ form was suggested to bind the amide formed after cleavage of the N_2 bond by the lithium metal. The lithium atom−nitrogen molecule reaction, studied by codepositing lithium and nitrogen at 15 K,[9] results in two absorptions at 1800 and 1535 cm^{-1} for NN fundamental vibrations. These were assigned to LiN_2 (lithium supernitride) and to $N_2Li_2N_2$ (lithium disupernitride), based on molecular orbital computations and the analysis of nitrogen isotope data. The 1535 cm^{-1} band was assigned to a species containing two N_2 units, and the 1800 cm^{-1} absorption probably was due to a product with a single lithium.

In view of the fact that lithium metal reacts with N_2 to form lithium nitride (Li_3N), a reversible hydrogen storage candidate,[10] even at room temperature, we wondered how and to what extent small Li clusters might be able to activate N_2. These clusters might serve as helpful models for the combustion of lithium in nitrogen gas and help guide studies of the reaction of N_2 with lithium metal surfaces.

2. Computational Methods

The geometries of all the complexes, reactants, intermediates, transition states, and products were optimized at the Density Functional Theory level, using hybrid-GGA B3LYP[11] functional and ultrafine integration grids as defined in Gaussian 03[12] and the standard 6-311+G* basis set in its spherical harmonic expression. The aug-cc-pVDZ basis was used to compute natural charges. Analytical computation of harmonic vibrational frequencies characterized stationary points and gave the zero-point energies. Intrinsic reaction coordinate (IRC) calculations on all transition structures confirmed the associated reactants and products.[13] MP2 computations were performed for critical cases, e.g., the key exothermic steps for the reduction of double the single NN bonds, the exothermicity of the $N_2 + Li_8$ reaction, etc. In addition, CCSD(T,fc)/6-311+G* single-point computations on the B3LYP/6-311+G* geometries of all the stationary points on the N_2Li_2, N_2Li_4, N_2Li_6, and N_2Li_8 potential energy surfaces were carried out. Additional X3LYP results are not reported, as they were not significantly better than those at B3LYP.

The potential energy surfaces were explored using Saunders' stochastic search "kick" method,[14a] which facilitates thorough exploration of chemically nonintuitive minima with very little human effort.[14b,c] "Kick" places all the atoms at the same point initially and displaces them randomly within a box of chosen dimensions. The kick size was varied from 2.0 to 3.5 Å in the cubic boxes employed here. A total of 2000 kick jobs in independent sets of 100 were performed at the HF/STO-3G level of theory. Redundancies in each set (energies within 0.000 01 au) are eliminated. The sets of kick runs were continued until no new structures were generated. The best structures from the initial level were then reoptimized at the B3LYP/6-311+G* level. Natural population analysis implemented in NBO 5.0[15] gave natural atomic charges and revealed the high ionic character of the electron distributions in the N_2Li_n ($n = 6, 8$) complexes. The Gaussian03 program was employed for all computations.[12]

3. Results and Discussion

3.1. Revisiting the 1972 Experiment of Andrews et al. There is only one prior investigation directly related to the subject of our study, the reaction of N_2 with lithium clusters: the 1972 matrix isolation study by Andrews et al.[9] of the interaction of lithium atoms codeposited with nitrogen molecules at 15 K. Infrared spectroscopic observation of two absorptions at 1800 and 1535 cm^{-1} for NN fundamental vibrations suggested the formation of two lithium−nitrogen species, LiN_2 ("lithium supernitride") and $N_2Li_2N_2$ ("lithium disupernitride"), the latter containing two equivalent N_2 units. Structures were not assigned. The authors proposed that the dinitrogen moiety in the observed lithium−nitrogen species is reduced more than in N_2 transition metal complexes, where the NN modes are higher (~2000 cm^{-1}) (for example, the NN IR stretch is 1955 cm^{-1} in $[(depe)_2Fe(N_2)]$ (depe = $Et_2PCH_2CH_2PEt_2$).[5d]

Using the stochastic "kick" procedure (see above), we reinvestigated the supernitride LiN_2 and disupernitride Li_2N_4 potential energy surfaces. The good match of the experimental with our computed stretching frequencies suggested several alternative structural candidates for the products, two for LiN_2 and four for Li_2N_4 (Figure 1).

The NN bond lengths for the several C_{2v}, C_{2h}, and C_1 symmetry Li_2N_4 minima we found ranged from 1.161 to 1.237 Å (**1**−**6**, Figure 1). The four lowest energy stationary points (**1**−**4**) have relative energies within ~5.5 kcal/mol. The computed (B3LYP/6-311+G*) NN IR stretching frequencies of the Li_2N_4 species **1**−**4** are 1784, 1793, 1488, and 1515 cm^{-1}, respectively (a 0.98 scaling factor was applied).[16] However, two other NN stretching frequencies, 2230 and 2154 cm^{-1}, for stationary points **3** and **4** (N_2 complexed with N_2Li_2 moiety in side on and end on fashion), were not observed experimentally. Evidently, a mixture of Li_2N_4 species might have been formed in Andrews' 1972 experiment. The fundamental NN stretching vibration corresponding to one of the computed structures (**4**, 1515 cm^{-1}, with a *side-on* N_2 complexed with the D_{2h} planar N_2Li_2 moiety) is closest to the experimentally observed N−N fundamental vibration (1535 cm^{-1}) of Li_2N_4 species. However,

(7) (a) Gambarotta, S. *J. Organomet. Chem.* **1995**, *500*, 117–126. (b) Gambarotta, S.; Scott, J. *Angew. Chem., Int. Ed.* **2004**, *43*, 5298–5308. (c) Schrock, R. R. *Angew. Chem., Int. Ed.* **2008**, *47*, 5512–5522, and references therein. (d) Curley, J. J.; Cook, T. R.; Reece, S. Y.; Müller, P.; Cummins, C. C. *J. Am. Chem. Soc.* **2008**, *130*, 9394–9405. (e) Tanaka, H.; Mori, H.; Seino, H.; Hidai, M.; Mizobe, Y.; Yoshizawa, K. *J. Am. Chem. Soc.* **2008**, *130*, 9037–9047. (f) Fryzuk, M. D. *Acc. Chem. Res.* **2009**, *42* (1), 127–133. (g) Schenk, S.; Reiher, M. *Inorg. Chem.* **2009**, *48* (4), 1638–1648. (h) Mori, M. *Heterocycles* **2009**, *78* (2), 281–318. (i) Christian, G.; Stranger, R.; Yates, B. F. *Chem.—Eur. J.* **2009**, *15* (3), 646–655.
(8) Mori, M.; Hori, K.; Akashi, M.; Hori, M.; Sato, Y.; Nishida, M. *Angew. Chem., Int. Ed.* **1998**, *37*, 636–637.
(9) Spiker, R. C.; Andrews, L., Jr.; Trindle, C. *J. Am. Chem. Soc.* **1972**, *94*, 2401–2407.
(10) (a) Chen, P.; Xiong, Z.; Luo, J.; Lin, J.; Tan, K. L. *Nature* **2002**, *420*, 302–304. (b) Palumbo, O.; Paolone, A.; Cantelli, R.; Chandra, D. *Int. J. Hydrogen Energy* **2008**, *33*, 3107–3110.
(11) (a) Becke, A. D. *Phys. Rev. A* **1988**, *38*, 3098–3100. (b) Lee, C.; Yang, W.; Parr, R. G. *Phys. Rev. B* **1988**, *37*, 785–789.
(12) Frisch, M. J. *Gaussian 03*, revision C.02; Gaussian, Inc.: Wallingford, CT, 2004.
(13) Fukui, K. *Acc. Chem. Res.* **1981**, *14*, 363–368.
(14) (a) Saunders, M. *J. Comput. Chem.* **2004**, *25*, 621–626. (b) Bera, P. P.; Sattelmeyer, K. W.; Saunders, M.; Schaefer, H. F.; Schleyer, P. v. R. *J. Phys. Chem. A* **2006**, *110*, 4287–4290. (c) Roy, D.; Corminboeuf, C.; Wannere, C. S.; King, R. B.; Schleyer, P. v. R. *Inorg. Chem.* **2006**, *45*, 8902–8906.
(15) Reed, A. E.; Curtiss, L. A.; Weinhold, F. J. *Chem. Rev.* **1988**, *88*, 899–926.
(16) Scott, A. P.; Radom, L. *J. Phys. Chem.* **1996**, *100*, 16502–16513.

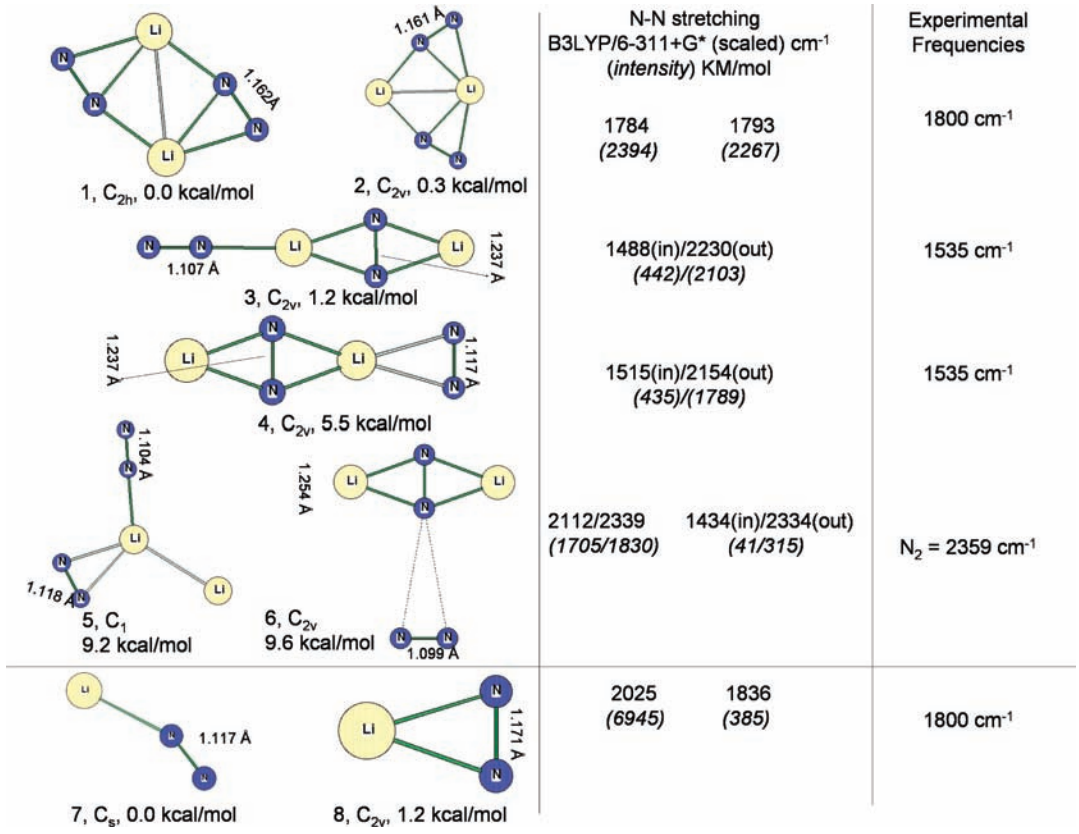

Figure 1. B3LYP/6-311+G* geometries and relative energies, N−N stretching frequencies (cm^{-1}), and intensities (KM/mol) for LiN_2 and Li_2N_4 species.

not only our computed scaled 1779 cm^{-1} NN stretching frequency of the C_{2v} triangular LiN_2 species (**8**) but also the 1783 and 1793 cm^{-1} frequencies for **1** and **2**, respectively, correspond to the experimentally observed 1800 cm^{-1} N−N frequency assigned to a "lithium−nitrogen" species with a single lithium (Figure 1). At the single-point CCSD(T)/6-311+G*//B3LYP/6-311+G* level, a C_s bent Li−N−N structure (**7**) is 15 kcal/mol higher in energy than LiN_2 (**8**, C_{2v}). Moreover, although **7** is slightly lower in energy than the C_{2v} form (**8**) at B3LYP, its computed scaled stretching frequency (2024 cm^{-1}) was not observed experimentally.

3.2. Reaction of N_2 with Li_2 and Li_4 Clusters. The LiN_2 and Li_2N_4 species discussed above are not likely to be key intermediates in the reactions of lithium clusters with nitrogen at room or higher temperatures. Lithium nitride, $(Li_3N)_x$, evidently forms by a series of reductive insertion steps whereby N_2 migrates into lithium clusters.

We now report computed mechanistic details of step-by-step insertion reactions of N_2 into lithium cluster models leading to dinitrogen reductions that convert N_2^0 into 2 N^{3-}. The oxidation number, which characterizes the degree of formal reduction of each nitrogen, ranges from zero in N_2, to −1 in LiNNLi, to −2 in the "hydrazido" Li_2NNLi_2, and to −3 in the "nitrido" NLi_3 (or its oligomers) corresponding to complete N−N cleavage.

The reaction of N_2 with Li_2, investigated for orientation (see Figure 2 for the B3LYP/6-311+G* reaction profile), is endothermic, has a high barrier, and takes place with slight NN bond elongation. Clearly, larger Li clusters are needed to model the reduction process. The final product (D_{2h} N_2Li_2) is 1.3 kcal/mol higher in energy than the initial N_2 and Li_2 complex. The doubly bridged D_{2h} N_2Li_2 product resembles the binding mode of N_2 with Li_2 in $[Cp_2Zr(\mu\text{-PPh})]_2[\{(thf)_3Li\}_2(\mu\text{-}N_2)]$, a very rare

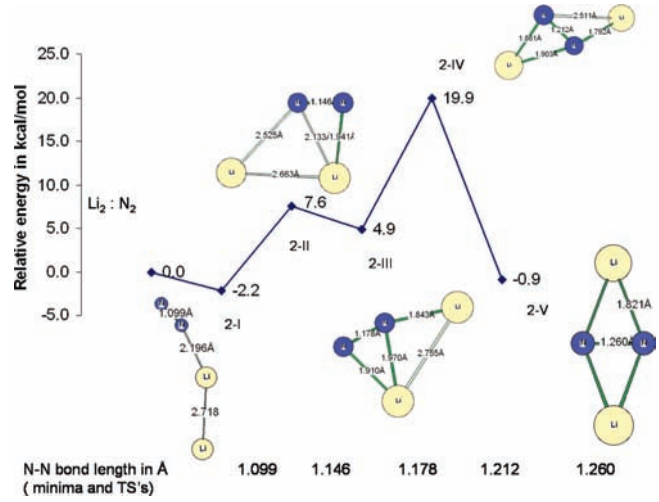

Figure 2. Pathway for the insertion of N_2 into the $D_{\infty h}$ Li_2 cluster showing intermediates and transition structures. Energies (ΔE, in kcal/mol at B3LYP/6-311+G*, ultrafine grid) are relative to the initial complex. The final D_{2h} N_2Li_2 rhombic complex is 1.3 kcal/mol higher in energy than the Li_2 and N_2 complex.

experimental example, featuring two Li atoms side-on bonded to a N_2 unit.[17] The reported N_2 bond length in the complex was very short [1.06(1) Å], hardly distinguishable from that in N_2 itself. The bonding interaction between Li and N_2 was attributed to the overlap of the Li(2s) and N(2s) orbitals based on ab initio molecular orbital calculations on a model dication system

(17) Ho, J.; Drake, R. J.; Stephan, D. W. *J. Am. Chem. Soc.* **1993**, *115*, 3792–3793.

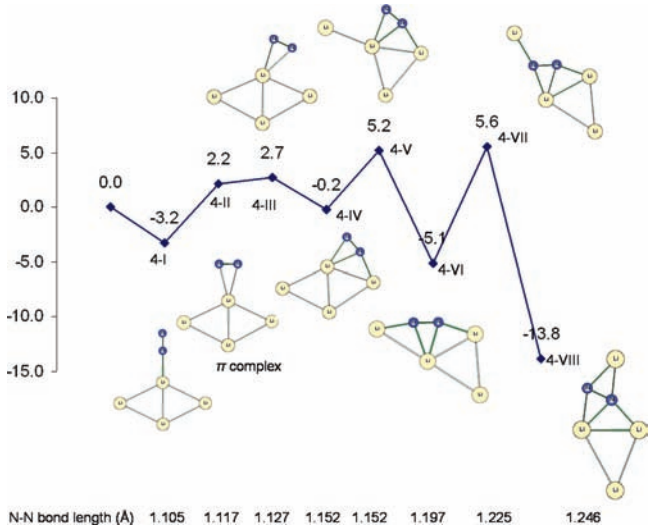

Figure 3. Pathway for the insertion of N_2 into the D_{2h} Li_4 cluster showing intermediates and transition structures. Energies (ΔE) relative to the initial complex are in kcal/mol (B3LYP/6-311+G*, ultrafine grid). The nomenclature employed here and in the subsequent Figures 5−7 designates the number of lithium atoms in Arabic numerals, followed by Roman numerals, e.g., **4-VIII**.

$[((H_2O)_3Li)_2(\mu\text{-}N_2)]^{2+}$. Our computed vibrational spectrum for the N_2Li_2 rhombic structure gave one relatively intense frequency (793 cm^{-1}; intensity 155 KM/mol), but the 1410 cm^{-1} stretching frequency is *infrared inactive*.

Since more lithium atoms are needed to achieve full reduction, we next investigated the reaction of N_2 with the planar D_{2h} Li_4 cluster to ascertain the geometrical changes along the reduction pathway. The binding energy of the side-on bound (C_{2v}) complex is ∼5 kcal/mol. The reaction profile is depicted in Figure 3. Several in-plane Li atom movements eventually lead to a formal dianion unit (N_2^{2-}). The N−N bond length in C_s N_2Li_4 (1.246 Å) is significantly longer than that in bare N_2 (1.096 Å). However, dinitrogen can only be activated partially with four lithium atoms; the final product bond length corresponds to a N=N double bond (cf., N−N = 1.235(6) Å, for the experimentally isolated $\{[Me_3SiNC(Ph)—NSiMe_3]_2V\}_2(\mu\text{-}\eta^1\text{:}\eta^1\ N_2)$).[18] Both (**4-VIII**), the global minimum on the N_2Li_4 PES, and (**4-IV**), another stationary point (see Figure 3), have characteristically intense N−N stretching frequencies: 1492.5 cm^{-1} (intensity 189.5 KM/mol) and 1699.1 cm^{-1} (intensity 179.5 KM/mol), respectively.

3.3. Migratory Insertion of N_2 in Li_6 and Li_8 Cluster. Since four lithium atoms are not sufficient to achieve full reduction, we investigated the mechanistic pathway for N_2 insertion into Li_6 clusters. Unlike N_2Li_4, finding all possible N_2Li_6 complexes is nontrivial. The N_2Li_6 potential energy surface (PES) was searched using Saunders' stochastic "kick" procedure (described in Computational Methods).[13] The plethora of interesting N_2Li_6 geometries obtained (see Figure 4) illustrates the well-precedented complexities of lithium structures.[19] While lithium−nitrogen bonding is largely ionic and bridging is common, the Li cluster moieties have their own preferences.[6i] The structures in Figure 4 obtained with "kick" either are planar (with NN bond lengths ranging from 1.105 to 1.241 Å) or are three-dimensional (with 1.106 to 1.574 Å NN lengths).

The bare D_{2h} Li_6 lithium cluster is 4.8 kcal/mol lower in energy than planar D_{3h} Li_6. Similarly, the apex-bound N_2Li_6 complex (**K6-V**) is 11.6 kcal/mol more stable than its planar C_s counterpart (**K6-I**), and the side-bound nonplanar C_1 N_2 complex (**K6-VI**) is 6.1 kcal/mol lower in energy than the analogous planar C_s minimum (**K6-II**) (Figure 4). As no planar minimum has NN separations greater than 1.25 Å, we concentrated on the nonplanar alternatives.

An energetically viable stepwise mechanism modeling reduction to a nitrido product, $(NLi_3)_2$, starts from the C_{4v} N_2−Li_6 complex (**6-I/K6-V**) and is depicted in Figure 5. The 8.9 kcal/mol exothermicity of the initial complex formation surmounts the subsequent small reaction barriers for the first stage of NN bond elongation to over 1.2 Å. Several out-of-plane Li atom movements but very little additional activation is needed to give a local minimum (**6-VIII**) with a 1.25 Å NN length and the hydrazido (D_{2h}) N_2Li_6 global minimum (**6-XII**) with *r*NN 1.487 Å.[15]

Unexpectedly, the fully reduced N_2Li_6 nitrido compound, a $[(NLi_3)_2]$ complex (**6-XIV**, Figure 5), with a 3.190 Å separation, is 5.5 kcal/mol higher in energy than (**6-XII**).[20] In addition, a large activation barrier (27.6 kcal/mol) hinders the conversion of the hydrazido (**6-XII**) to the nitrido form (**6-XIV**). The N−N bond order of the N_2Li_6 global minimum (**6-XII**) is lower than one, and the N−N stretching frequency is 788 cm^{-1} (intensity 56 KM/mol). The stationary point (**6-X**) has essentially has the same N−N bond length (1.440 Å) and the N−N stretching frequency is similar (810 cm^{-1}; intensity 120 KM/mol).

This problem of incomplete reduction (only to oxidation number −2) is not encountered when two additional lithiums are included. The N_2Li_8 PES, explored using the "kick" stochastic search method,[13] has numerous interesting minima with NN bond lengths ranging from 1.1 to over 3 Å (see Figure 6).

Our mechanism for nitrogen insertion into the most stable Li_8 cluster isomer, known to have T_d symmetry,[21] is shown in Figure 7. The starting side-on-bound N_2Li_8 complex (**8-I**), with N_2 (r = 1.111 Å) extending from one of the T_d Li_8 edges, is lower in energy than the end-on-bound alternatives (not shown). However, as depicted in Figure 7, side-on complexes are involved in the N_2 insertion. As with N_2Li_6 (see Figure 5), the initial reaction profile is rather flat with many minima having similar energies. Precedents for such cluster variants involving lighter metals are well-known.[6i] The final fully reduced N_2Li_8 nitrido product (**8-XVIII**) with well-separated N atoms (*r*NN = 3.023 Å) not only is the global minimum but also is 82.4 kcal/mol more stable than the weakly N_2 bound starting complex (**8-I**)! This N_2Li_8 pathway is much more exothermic than that for N_2 insertion into Li_6 (compare Figure 5), where nitrido N_2Li_6 (**6-XIV**) is only 30.2 kcal/mol lower in energy than the initial complex, and is not the global minimum N_2Li_8.

We also report stretching frequencies for some of the N_2Li_8 local minima, which might be verified by experiment. Structures **8-XI** and **8-XIII** have greater N−N separations than typical

(18) Hao, S.; Berno, P.; Minhas, R. K.; Gambarotta, S. *Inorg. Chim. Acta* **1996**, *244*, 37–49.

(19) (a) Dill, J. D.; Schleyer, P. v. R.; Binkley, J. S.; Pople, J. A. *J. Am. Chem. Soc.* **1977**, *99*, 6159–6173. (b) Schleyer, P. v. R. *Pure Appl. Chem.* **1984**, *56*, 151–162. (c) Gregory, K.; Schleyer, P. v. R.; Snaith, R. *Adv. Inorg. Chem.* **1991**, *37*, 47–142. (d) Glukhovtsev, M. N.; Schleyer, P. v. R. *Isr. J. Chem.* **1993**, *33*, 455–466. (e) *Lithium Chemistry: A Theoretical and Experimental Overview*; Sapse, A.-M., Schleyer, P. v. R., Eds.; Wiley: New York, 1995. (f) Wheeler, S. E.; Sattelmeyer, K. W.; Schleyer, P. v. R.; Schaefer, H. F. *J. Chem. Phys.* **2004**, *120*, 4683–4689.

(20) The relative energy is 5.2 kcal/mol with CCSD(T)/aug-ccpVDZ single-point calculation (at the MP2/6-311+G* geometry).

(21) Gardet, G.; Rogemond, F.; Chermette, H. *J. Chem. Phys.* **1996**, *105*, 9933–9947.

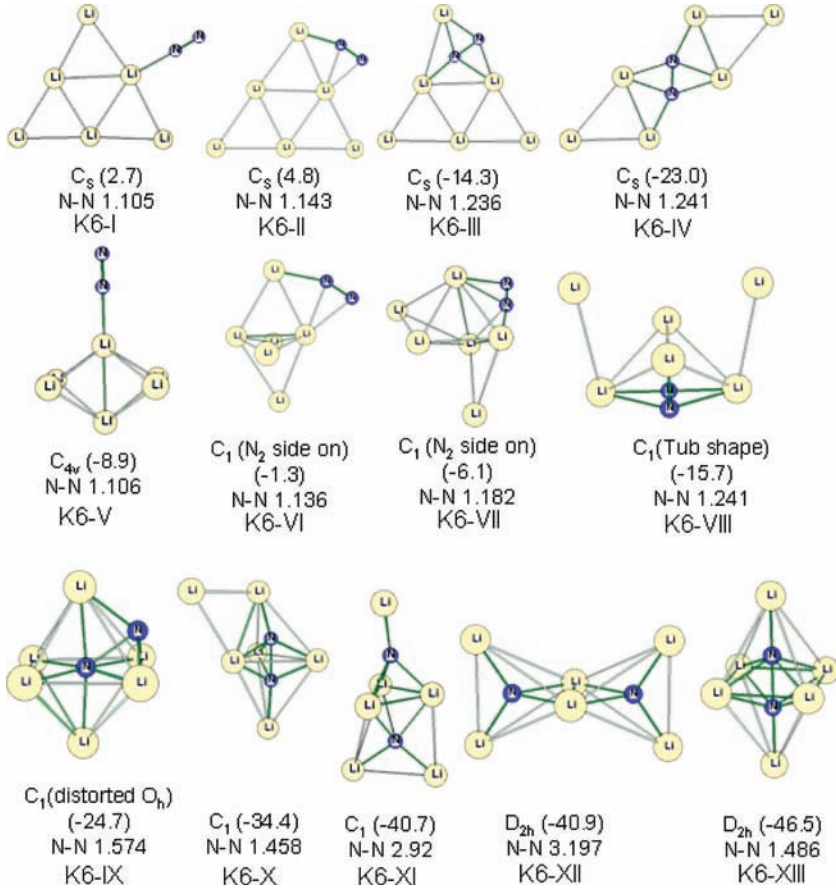

Figure 4. N_2Li_6 minima obtained from "kick" (designated by the prefix K) with various NN distances (in Å) located by stochastic searches (B3LYP/6-311+G* energies in kcal/mol relative to separated N_2 + Li_6 are given in parentheses).

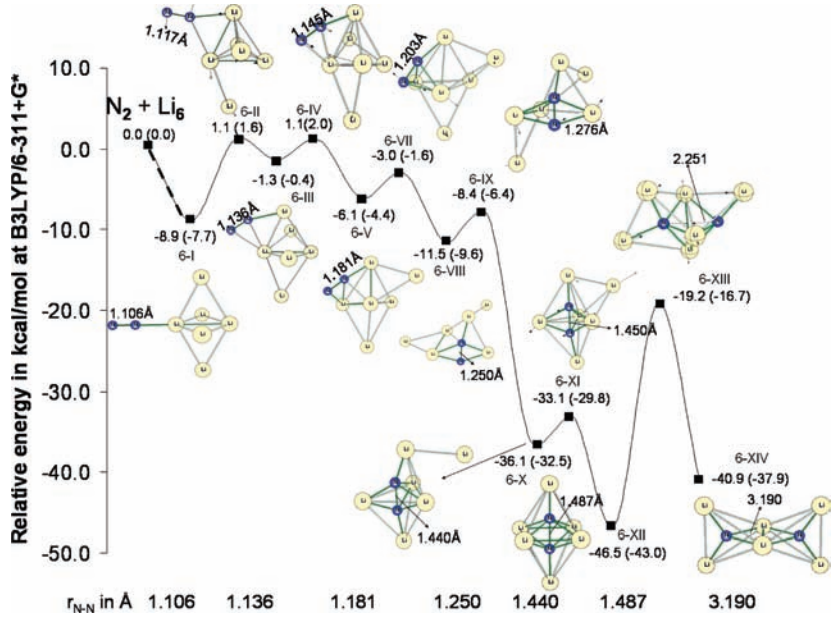

Figure 5. Pathway for the N_2 insertion into a Li_6 cluster. Structures of transition states, intermediates, and products are shown (B3LYP/6-311+G*, ultrafine grid). The zero-point vibrational energy corrected energies (ZPVE) are reported in parentheses.

N—N single bond lengths [1.454 Å], whereas **8-VII** and **8-IX** have N═N double bond distances. The B3LYP/6-311+G* stretching frequencies (in cm^{-1}) and intensities [KM/mol] are **8-VII** (1308 [154]), **8-IX** (1248.5 [304]), **8-XI** (756 [288]), and **8-XIII** (640 [55]).

3.4. Validation of Hybrid Density Functional Approach. We carried out CCSD(T) single-point computations on B3LYP geometries on all the stationary points on the N_2Li_2, N_2Li_4, N_2Li_6, and N_2Li_8 PESs (Table 1), following a reviewer's suggestion. The CCSD(T)/6-311+G* and the DFT results for

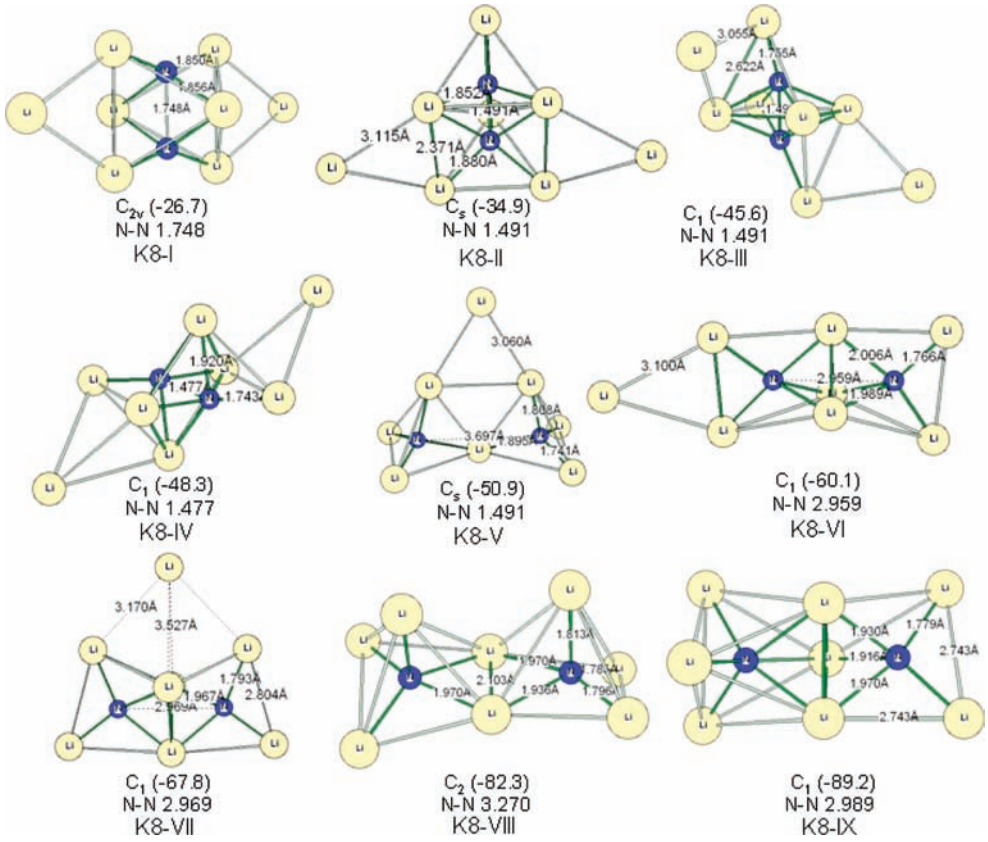

Figure 6. N_2Li_8 [minima] with various NN distances (in Å) located by stochastic searches. B3LYP/6-311+G* energies in kcal/mol relative to separated N_2 and Li_8 are given in parentheses.

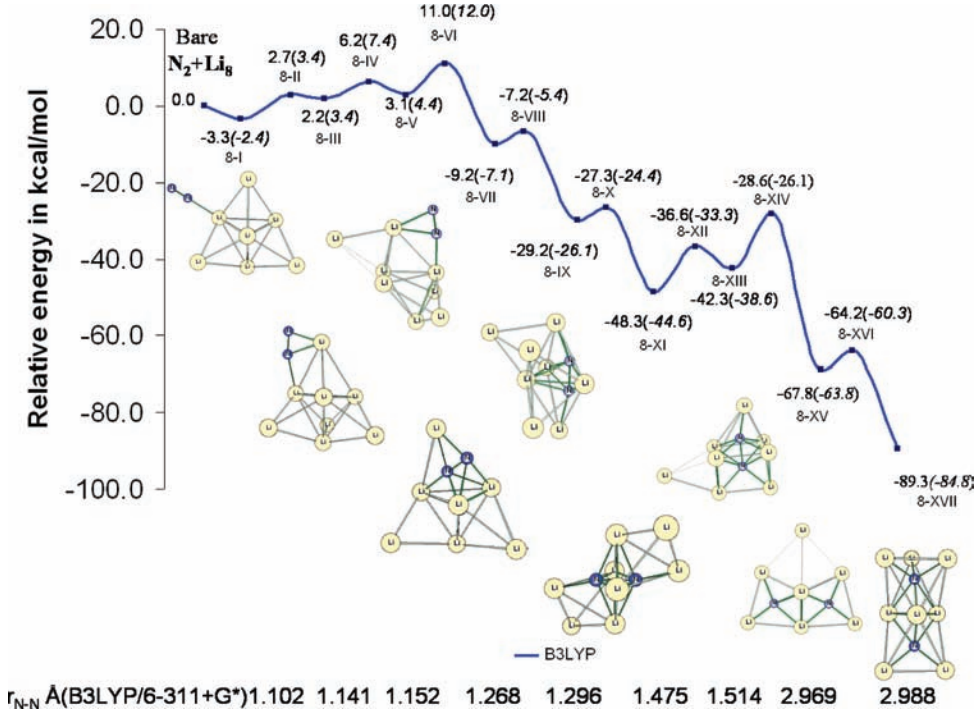

Figure 7. B3LYP/6-311+G* reaction profile for the insertion of N_2 into Li_8 cluster. Only the structures and the N−N bond lengths of the minima are depicted. The zero-point vibrational energy (ZPVE) corrected energies are reported in parentheses.

the most important N_2Li_6 and N_2Li_8 systems agree reasonably well numerically, and the qualitative energy ordering is the same. For example, the fully reduced N_2Li_6 nitrido compound (**6-XIV**), a $[(NLi_3)_2]$ complex, is 4.4 kcal/mol higher in energy than **6-XII** (compared to 5.5 kcal/mol at B3LYP/6-311+G*). Similarly, N_2Li_8, the global minimum, is 18.6 kcal/mol lower in energy than **8-XV** (compared to 21.5 kcal/mol at B3LYP/6-311+G). The CCSD(T) and B3LYP results do not agree for the N_2Li_4

Table 1. CCSD(T)/6-311+G*//B3LYP/6-311+G* Single-Point Relative Energies of the Stationary Points on N_2Li_2, N_2Li_4, N_2Li_6, and N_2Li_8 PESs[a]

N_2Li_2		N_2Li_4		N_2Li_6		N_2Li_8	
	CCSD(T)/6-311+G(2df) (single point) (kcal/mol)		CCSD(T)/6-311+G(d) (single point) (kcal/mol)		CCSD(T)/6-311+G(d) (single point) (kcal/mol)		CCSD(T)/6-311+G(d) (single point) (kcal/mol)
2-I	-2.7	4-I	-4.8	6-I	-5.7	8-I	-2.2
2-II	17.7	4-II	2.8	6-II	6.5	8-II	10.9
2-III	14.4	4-III	6.8	6-III	8.0	8-III	13.0
2-IV	25.5	4-IV	6.0	6-IV	10.7	8-IV	18.4
2-V	16.7	4-V	4.6	6-V	5.4	8-V	15.1
(Endothermic!)		4-VI	6.9	6-VI	8.7	8-VI	20.0
		4-VII	15.2	6-VII	4.8	8-VII	9.9
		4-VIII	-0.6	6-VIII	10.5	8- VIII	10.4
		(Overall endothermic!)		6-IX	-11.7	8-IX	-8.5
				6-X	-8.8	8-X	-5.2
				6-XI	-20.2	8-XI	-23.4
				6-XII	Did not converge	8-XII	-11.8
				6-XIII	-15.8	8-XIII	-16.2
						8-XIV	-7.0
						8-XV	-41.0
						8-XV	-37.6
						8-XVII	-59.6

[a] The energies are relative to separated N_2 + Li_n species.

Table 2. Variation of N—N Bond Lengths and Charges for the Important Stationary Points on the N_2Li_6 and N_2Li_8 Reaction Profiles Resulting from Step-by-Step Reduction of Dinitrogen with Six and Eight Lithium Atoms, Respectively

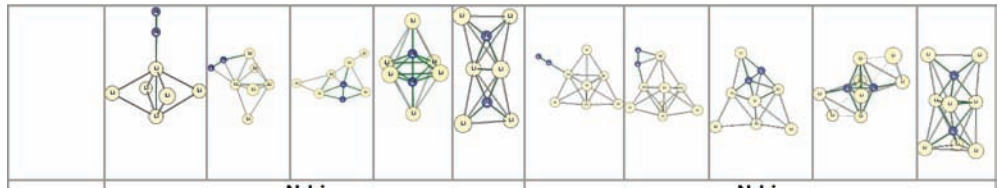

	N_2Li_6					N_2Li_8				
N-N Bond Length (Å)	1.106	1.136	1.250	1.487	3.190	1.111	1.148	1.273	1.483	3.023
NBO Charge[a] (N_1)	-0.168	-0.371	-1.048	-1.802	-2.786	-0.153	-0.365	-1.081	-1.742	-2.855
(N_2)	0.005	-0.116	-0.703	-1.802	-2.787	0.019	-0.268	-0.905	-1.742	-2.813

[a] Charge from natural population analysis at B3LYP/aug-ccpVDZ.

complexes, but this aspect of our work is of lesser importance. The overall insertion reaction of N_2 into the Li_4 cluster is endothermic according to CCSD(T). The final product is 4.2 kcal/mol higher in energy than the sigma complex **4-I**. The B3LYP/6-311+G* N_2Li_4 PES may not be reliable as one of the local minima has an instability; triplet (**4-VI**) is only 1.8 kcal/mol higher in energy than the singlet. However, as a general trend, the reaction energies are too exothermic in the DFT computations. For instance, B3LYP predicts D_{2h} N_2Li_2 formation to be slightly exothermic, whereas CCSD(T) finds this reaction to be endothermic by ~17 kcal/mol.

The performance of the different methods was assessed by computing the atomization energies (AEs) of N_2, Li_2, NLi_3, and N_2Li_2 as well as the reaction energies of $N_2 + Li_2 \rightarrow N_2Li_2$ and $^1/_2\ N_2 + {}^3/_2\ N_2Li_2 \rightarrow NLi_3$ at MP2, CCSD(T), and G3B3 levels of theory as well as DFT with a variety of different GGA and hybrid-GGA functionals (the results are in the Supporting Information, SI. Tables 1 and 2). Most functionals overestimate the exothermicity for lithium nitride formation. These DFT errors are mainly due to overestimation of the binding energy of NLi_3 and N_2Li_2 and underestimation of the Li_2 binding energy. The good performance of the OLYP functional, which includes Handy's OPTX nonhybrid exchange functional, is notable.[22]

3.5. Analysis of Dinitrogen Activation during Step-by-Step Migratory Insertion. The extent of dinitrogen activation during the step-by-step insertion processes can be evaluated by well-defined observable properties like NN bond lengths or NN stretching vibrational frequencies. Experimental NN bond lengths generally are used for comparison purposes, e.g., 1.097 Å for the gaseous N_2 triple bond, 1.236 and 1.255 Å for the N═N double bond (in $\{[Me_3SiNC(Ph)\text{-}NSiMe_3]_2V\}_2(\mu\text{-}\eta^1\text{:}\eta^1\ N_2)$ and PhN═NPh, respectively), and 1.454 Å for the N—N single bond (hydrazine NH_2—NH_2).[2] The longest dinitrogen bond distance reported crystallographically (1.525(4) Å) is equivalent

(22) Handy, N. C.; Cohen, A. J. *Mol. Phys.* **2001**, *99*, 403–412.

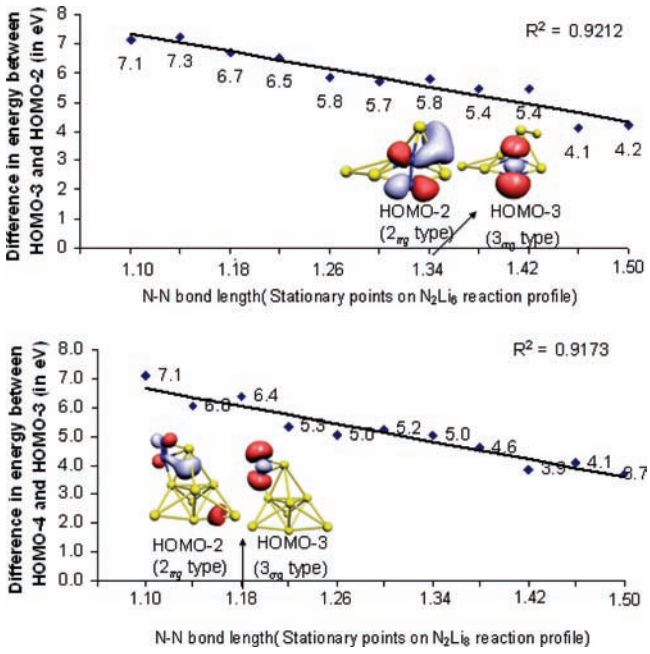

Figure 8. Linear relationship between the NN bond length elongation and decrease in the energy gap between the $2\pi_g$ and $3\sigma_g$ molecular orbitals of the N_2 moieties of the N_2Li_6 and N_2Li_8 clusters. Representative MOs are shown for one complex in each case.

to a long single bond and occurs in a hybrid complex of an alkali metal with a lanthanide (samarium(II)).[23] Additional criteria, such as partial charges, also can serve as descriptors. Note the successive increase in the N—N bond lengths, which correlates with the partial negative charges on the N atoms for the selected N_2Li_6 and N_2Li_8 stationary points in Table 2.

The tendency of lithium atoms to donate their valence electrons also is evident from the charge data. Moreover, the very large HOMO ($3\sigma_g$)−LUMO($2\pi_g$) gap for molecular dinitrogen (22.9 eV), which contributes to its inertness, is reduced substantially by the donation of electrons from lithium to the $2\pi_g$ orbitals. The stepwise reduction/bond elongation of dinitrogen is linearly related to the energy gap between $2\pi_g$ and $3\sigma_g$ type orbitals for both the N_2Li_6 and N_2Li_8 complexes (Figure 8). The N_2Li_6 and N_2Li_8 species with various NN bond lengths exhibit different degrees of N_2 reduction.

3.6. Exceptional Reactivity of N_2 with Lithium. Why does Li (but not Na and K) react with N_2 even at room temperature? The computed atomization energies (AE) of all the largely electrostatically bound species: BM_3 (D_{3h}), $BM_2(2)$($D_{\infty h}$), BM_4 (2)(C_1), $CM_2(2)$ (C_{2v}), $CM_3(2)$ (D_{3h}), CM_4 (T_d), $NM_2(2)$ ($D_{\infty h}$), NM_3 (D_{3h}), $NM_4(2)$ (T_d), OM_2 ($D_{\infty h}$), $OM_3(2)$ (D_{3h}), $OM_4(2)$ (T_d), SiM_4 (C_{2v}), PM_3 (D_{3h}) (M = Li, K, Na), reveal that the Li compounds have, by far, the highest AEs/atom for NM_3, 52.6 (Li), 27.0 (Na), and 23.2 (K) kcal/mol. The bond length and AE data for these six compounds are summarized in Table 3 (the bond length and AE data for the remaining compounds are included in SI. Table 3).

Moreover, the lithium compounds have the shortest Li−B/C/O/N/Si/P bond lengths and the largest charge separations (see SI. Table 4). For example, the natural charges for of alkali metal first row element compounds (natural charges computed with NBO 5.0 at B3LYP/6-311+G*) on NM_3 (M = Li, Na, K) are as follows: Li/N (+0.93/−2.81), Na/N (+0.77/,23 > 2.32), K/N (+0.80/−2.42). The atomization energy plotted against e^2/R for alkali metal containing B, C, and N molecules (e = natural charge on M) gives a directly proportional relationship with e^2/R for each series. The higher atomization energy for Li compounds can be attributed to the strongly ionic character of the Li−B/C/N bond (Figure 9).

4. Conclusions

The reaction of the normally quite inert N_2 with lithium is remarkably facile. As shown by our computed results, N_2 readily forms complexes at various positions of Li_2, Li_4, Li_6, and Li_8 model clusters. These isomeric complexes interconvert over generally low barriers, but the extent of NN elongation varies with cluster size. The small Li_4 cluster only reduces N_2 to double bond lengths (ca. 1.25 Å). Further reduction to nitrogen oxidation states −2 and −3 only occurred with N_2Li_6 and with N_2Li_8. The key step, with both N_2Li_6 and N_2Li_8, involved the sudden, exothermic (ca. 20 kcal/mol) double (∼1.3 Å) to single (∼1.48 Å) NN bond length elongation. The final reduction stage separates the N atoms to over 3 Å and embeds them centrally in $(NLi_3)_2$ and $(NLi_4)_2$ dimer clusters. Although $(NLi_3)_2$ is not the global N_2Li_6 minimum, it is 37 ± 1 kcal/mol more stable than separated N_2 + Li_6 (at both B3LYP/6-311+G* and MP2/6-311+G*). The $(NLi_4)_2$ dimer end product is the N_2Li_8 global

Table 3. Atomization Energy/Alkali Metal Ratios (for BM_3, CM_4, NM_3, OM_2, PM_3, and SiM_4)[a]

	Li			Na			K		
	Bond length (Å)	AE kcal/mol	AE/atom kcal/mol	Bond length (Å)	AE kcal/mol	AE/atom kcal/mol	Bond length (Å)	AE kcal/mol	AE/atom kcal/mol
BM_3	2.133	94.7	31.6	2.511	63.1	21.0	2.932	48.8	16.3
CM_4	1.865	191.1	47.8	2.284	112.7	28.2	2.659	91.2	22.8
NM_3	1.722	157.8	52.6	2.159	81.1	27.0	2.414	69.6	23.2
OM_2	1.627	170.7	85.4	1.994	108.6	54.3	2.231	111.5	55.8
PM_3	2.218	141.4	47.1	2.593	97.4	32.5	2.924	85.1	28.4
SiM_4	2.342	148.5	37.1	2.703	105.8	26.5	3.092	90.7	22.7

[a] The Li compounds have highest AE/atom, ∼1.5 times those of Na and K, in accord with the unusual reactivity pattern of lithium among the alkali metals.[24]

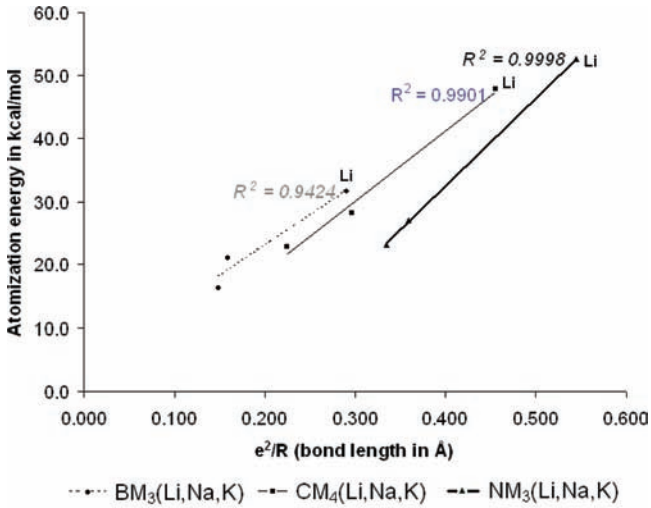

	e^2/R	AE/atom kcal/mol		e^2/R	AE/atom kcal/mol		e^2/R	AE/atom kcal/mol
BLi_3	0.290	31.6	CLi_4	0.455	47.8	NLi_3	0.545	52.6
BNa_3	0.159	21.0	CNa_4	0.296	28.2	NNa_3	0.359	27.0
BK_3	0.149	16.3	CK_4	0.225	22.8	NK_3	0.335	23.2

Figure 9. Plot of atomization energy vs e^2/R for alkali metal containing B, C, and N molecules (e = natural charge on M).

minimum; the exothermicity of the $N_2 + Li_8$ reaction is enormous, 81 ± 4 kcal/mol (B3LYP and MP2, ~60 kcal/mol at CCSD(T)). The exceptional reactivity of N_2 with lithium, compared to the other alkali metals, e.g., sodium and potassium, is clarified. Li is a very strong reducing agent as its nitrides have the highest atomization energies, the shortest M−N bond distances, and the largest M−N charge separations as well as interaction energies.

Our detailed mechanisms for the insertion of N_2 into model lithium clusters delineates the general manner in which molecular nitrogen can be activated sequentially by electron transfer and bond elongation, to give a series of increasingly reduced complexes. Lithium by itself is not a catalyst, but its incorporation into complexes might facilitate the development of a nitrogen fixation catalyst.

Acknowledgment. We thank the Research Computing Center of University of Georgia and the Centro de Supercomputación de Galicia for providing computational resources, Dr. Y. Yamaguchi for numerous scientific discussions, the University of Georgia for a Ph.D. Dissertation award stipend (to D. R.), the National Science Foundation Grant CHE-0716718 for financial support, and the Spanish Government for a Research Contract (to A.N.) in the framework of the "Ramón y Cajal" program.

Supporting Information Available: Geometries (*xyz*) and absolute energies (in hartree) for all the N_2Li_n stationary points and kick structures; full Gaussian 03 ref 12; table for bond lengths and natural charges for compounds of alkali metal first row and second row elements; table for the reaction energies of $N_2 + Li_2 \rightarrow N_2Li_2$ and $^1/_2\,N_2 + {}^3/_2\,N_2Li_2 \rightarrow NLi_3$ at OLYP, B3LYP, BLYP, PBEPBE, X3LYP, O3LYP, M05-2X, MP2, CCSD(T), and G3B3 levels of theory are included in the Supporting Information. This material is available free of charge via the Internet at http://pubs.acs.org.

JA902980J

(23) Jubb, J.; Gambarotta, S. *J. Am. Chem. Soc.* **1994**, *116*, 4477–4478.
(24) Clugston, M.; Flemming, R. *Advanced Chemistry*; Oxford University Press: Oxford, 2000; pp 294−296.